

Refreshable Braille Display System Based on Triboelectric Nanogenerator and Dielectric Elastomer

Xuecheng Qu, Xiu Ma, Bojing Shi, Hu Li, Li Zheng, Chan Wang, Zhuo Liu, Yubo Fan, Xiangyu Chen,* Zhou Li,* and Zhong Lin Wang

The blind mainly relies on Braille books to obtain text information. However, Braille books with invariable content are ponderous and inconvenient to read. Hence, it is essential to find a safe, simple and effective method to develop new Braille devices. This advanced method promises to be the next generation Braille book that is refreshable, flexible, and portable. Therefore, a safe dielectric elastomer Braille device actuated by a triboelectric nanogenerator is designed. It is easy to fabricate, inexpensive, and safe without any potential hazard for blind people. For triboelectric nanogenerators, the friction between two thin films can generate a voltage over 3 kV with a current of just 2 μA to deliver a shape change of the dielectric elastomer membrane. In the meantime, with the support of the pressor air in the chamber, the membrane will be raised up to be a touchable Braille dot. In addition, a programmed switch matrix is designed to control the Braille device with multiple dielectric elastomer dots to realize complicated refreshable display, providing a possibility of a page-size and portable braille e-book for the blind in the near future.

1. Introduction

According to data released by the World Health Organization, there are about 36 million blind people worldwide.^[1] By reason of impaired vision, the blind cannot learn and read like

the normal. They can only rely on touch, hearing and residual vision to obtain information about the environment. Braille is a kind of text specially designed for blind people. Each character is composed of 6 bumps arranged in three rows and two columns, which can be combined into different characters.^[2] Through the tactile perception of finger touch, blind people can obtain text information from the Braille book (Figure 1a). However, the recent commercial paper Braille books are too cumbersome to use, and the contents of the book cannot be refreshed, so that they cannot help the blind get real-time information.

Recently, a various new type of Braille display devices based on electroactive polymers and electronic techniques have been developed,^[3] including dielectric elastomer actuators monitored by flexible thin-film transistors,^[4] temperature-controlled bistable electroactive polymer,^[5] dielectric elastomer (DE) actuator coupled with water,^[6] and compact dielectric elastomer tubular actuator.^[7] Dielectric elastomer is an electroactive polymer that can produce large deformation under the electric field and returning to its original size immediately after

X. Qu, X. Ma, Dr. B. Shi, Dr. H. Li, C. Wang, Dr. Z. Liu, Prof. X. Chen, Prof. Z. Li, Prof. Z. L. Wang
CAS Center for Excellence in Nanoscience
Beijing Key Laboratory of Micro-nano Energy and Sensor
Beijing Institute of Nanoenergy and Nanosystems
Chinese Academy of Sciences
Beijing 100083, China
E-mail: chenxiangyu@binn.cas.cn; zli@binn.cas.cn


X. Qu, C. Wang, Prof. X. Chen, Prof. Z. Li, Prof. Z. L. Wang
School of Nanoscience and Technology
University of Chinese Academy of Sciences
Beijing 100049, China

X. Ma, Prof. L. Zheng
College of Mathematics and Physics
Shanghai Key Laboratory of Materials Protection and
Advanced Materials in Electric Power
Shanghai University of Electric Power
Shanghai 200090, China

Dr. B. Shi, Dr. H. Li, Dr. Z. Liu, Prof. Y. Fan
Beijing Advanced Innovation Centre for Biomedical Engineering
Key Laboratory for Biomechanics and Mechanobiology
of Ministry of Education
School of Biological Science and Medical Engineering
Beihang University
Beijing 100191, China

Prof. X. Chen, Prof. Z. Li
Center of Nanoenergy Research
School of Physical Science and Technology
Guangxi University
Nanning 530004, China

Prof. Z. L. Wang
School of Materials
Science and Engineering
Georgia Institute of Technology
Atlanta, GA 30332-0245, USA

 The ORCID identification number(s) for the author(s) of this article can be found under <https://doi.org/10.1002/adfm.202006612>.

DOI: 10.1002/adfm.202006612

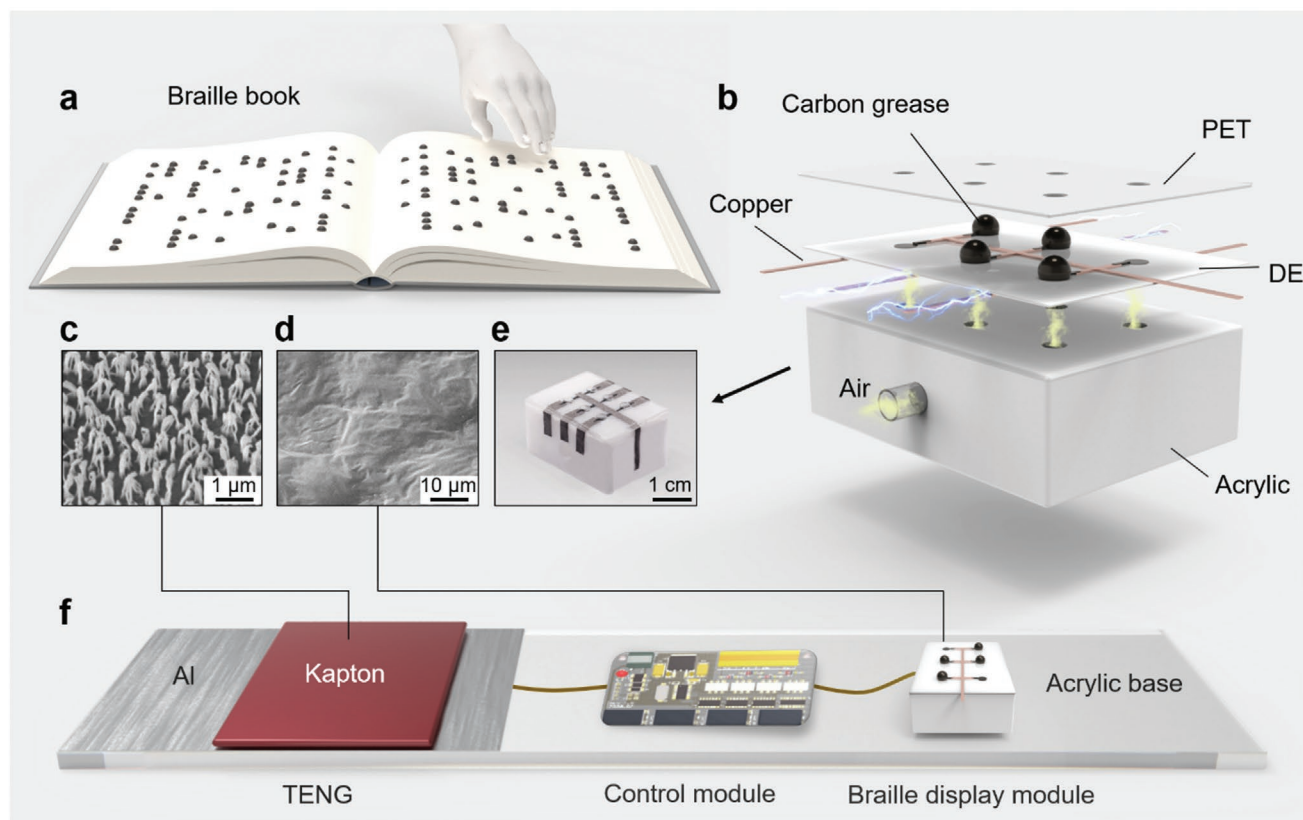


Figure 1. Design of the RBDS. a) Schematic diagram of a conventional Braille book. b) Exploded view of the Braille display module. c) SEM image of nanostructure on the surface of Kapton film treated by ICP reactive-ion etching. d) SEM image of the carbon grease on the DED. e) Photo of the Braille display module. f) Schematic diagram of the RBDS with control module.

the electric field being removed.^[8] Braille devices made from dielectric elastomer are flexible and refreshable, which can supply better tactile sensations and potentials to get real-time information. Some researchers have also developed other types of Braille display devices.^[9–12] However, these types of Braille devices are strongly dependent on high voltage (HV) supplies, which may pose potential dangers to the human body.

Triboelectric nanogenerators (TENGs) that can convert mechanical energy into electricity have been used in various fields, including energy harvesting,^[13–16] sensors,^[17–19] medical devices,^[20,21] rehabilitation,^[22] and so on.^[23] It is noteworthy that some interesting output properties of high voltage (kV magnitude) and low current (μA magnitude) are drawing attention from researchers.^[24,25] In addition, other advantages such as simple structure, easy fabrication and cost-effective make TENG suitable for acting as a convenient and safe HV power source,^[26] which have been used in molecular mass spectrometry^[27] and plasma source.^[28,29]

2. Results

2.1. Design of the Refreshable Braille Display System

We presented a refreshable Braille display system (RBDS) based on TENG and DE membrane. The central part of the

RBDS was a Braille display module consisted of dielectric elastomer dots (DEDs), flexible electrodes and an air chamber (Figure 1b). The DE membrane was stretchable (Figure S1, Supporting Information). The TENG acted as a HV source was made by an acrylic sheet, an Al foil and a Kapton film (Figure S2, Supporting Information). It is necessary to note that the sliding type TENG employed in this work is the simplest TENG mode.^[30] Since this work is the first report about Braille display based on TENG, this sliding type TENG is chosen for clearly revealing the working concept of the system. In future work, there are many other type TENGs with a more compact structure or simpler operation method that can be selected, such as the charge pumping type TENG,^[31] rotating type TENG,^[32] and so on.

To enhance the output performance of the TENG, inductively coupled plasma (ICP) reactive-ion etching^[33] was used to modify the surface of the Kapton film (Figure 1c). An output voltage of TENG over 3 kV can be achieved. The flexible electrodes made by carbon grease were applied to the upper and lower sides of the DED (Figure 1d). Compared with the metal electrode, the carbon grease electrode could follow the deformation of the DE membrane well without cracking (Figure S3, Supporting Information). A PET sheet with six holes was attached above the whole DE membrane to enhance the actuated effect and protect the Braille device. The size of the Braille display module is 30 mm \times 22 mm \times 16 mm

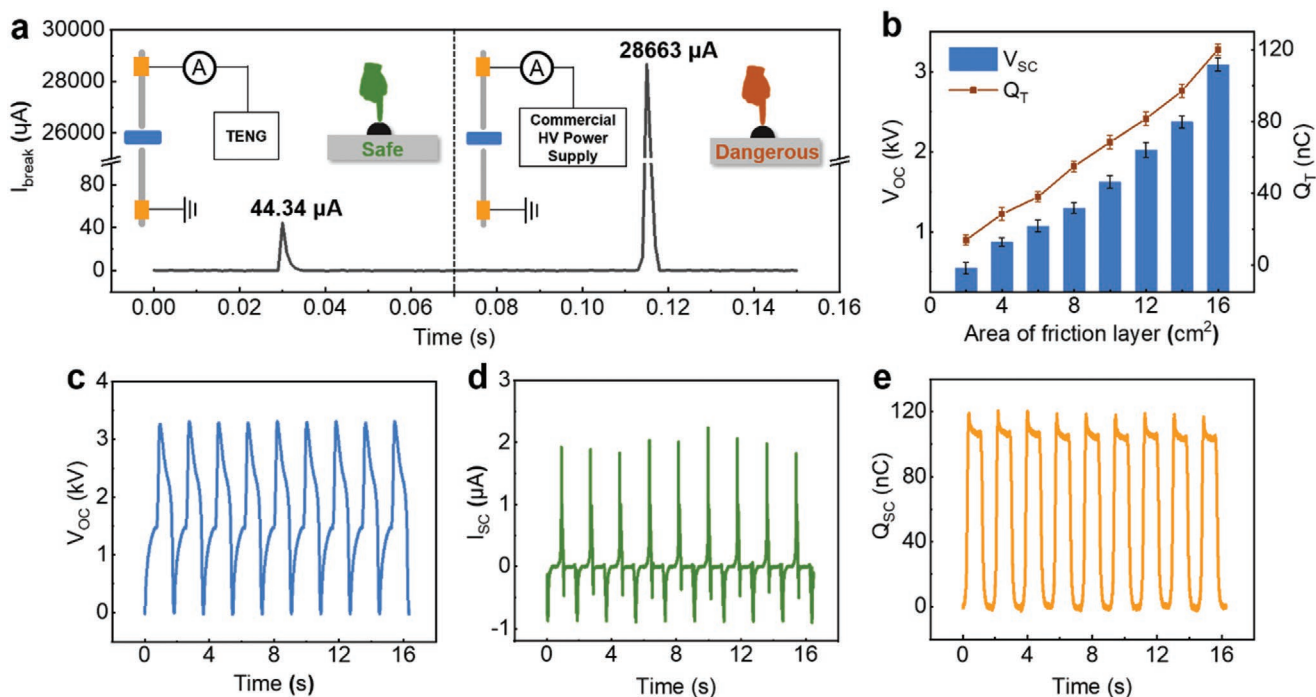


Figure 2. Electrical characterization of TENG. a) Breakdown current values of the DED actuated by TENG (16 cm² area) and commercial HV power, respectively, and schematic diagram of test connection. b) Open-circuit voltage and transfer charge of the TENG under different friction layer area. c) Open-circuit voltage of the TENG with area of 16 cm². d) Short circuit current of the TENG with area of 16 cm². e) Transferred charge of the TENG with area of 16 cm².

(Figure 1e). The control module with multiple I/O ports can perform multi-threaded control through programs, and then the RBDS can display different Braille characters with the control module. The Braille display module, the TENG and the control module together form the complete RBDS (Figure 1f).

2.2. Electrical Characterization of Triboelectric Nanogenerator

To better illustrate the advantage of the safety of the TENG, we measured the breakdown current (I_{break}) values of the DED actuated by the TENG and the commercial HV power, respectively (Figure 2a and Figure S4, Supporting Information). It can be found that the I_{break} caused by the TENG (44.34 μA) was far smaller than that of the commercial HV power (28663 μA), which was beyond the human body safety current (10 000 μA). It means that the TENG can be used as a safer high-voltage power supply. In addition, the outputs of the TENG with different areas were tested. The TENG was driven periodically by a linear motor with a frequency of 0.5 Hz. As the area of the TENG increased, the open-circuit voltage (V_{OC}) and the transferred charge (Q_{T}) would also increase (Figure 2b and Figure S5, Supporting Information). The peak value of the V_{OC} of the TENG with the area of 16 cm² can reach up to 3250 V (Figure 2c). The corresponding short circuit current (I_{SC}) and Q_{T} were 2.05 μA (Figure 2d) and 119 nC (Figure 2e), respectively.

2.3. Refreshable Braille Display System with Single Dielectric Elastomer Dot

The bottom and top carbon grease electrodes of the DED were connected to the Al foil of the TENG and the ground, respectively. The thickness of the DED with electrodes was 281.5 μm (Figure S6, Supporting Information). The fabrication of RBDS with single DED is mentioned in Experimental Section (Figure S7, Supporting Information). When sliding the Kapton slider on the Al foil, the morphology of the DED would be correspondingly changed (Figure 3a and Movie S1, Supporting Information).

The operation mechanism of the DED actuated by the TENG is expounded in Figure 3b. In the original state, Kapton film and Al foil fully overlapped and intimately contacted with each other. According to the triboelectric series, Kapton has stronger electronegativity than Al. Thus, electrons are injected from Al to Kapton during the sliding process, which results in positive net charge aggregating on the surface of the Kapton film and equivalent negative net charge aggregating on the surface of the Al foil. Once the Kapton film was sliding out of the Al foil, potential difference would appear between these two materials. The DE membrane connected between the Al foil and the ground would endure this potential drop due to its capacitance characteristics. The electron transfer from the electrode of DED to Al foil. The positive charge accumulated at the bottom electrode of the DED and the negative charge accumulated at the top one. The electrostatic force created by the mutual attraction of the two charges would stretch the DE membrane in the

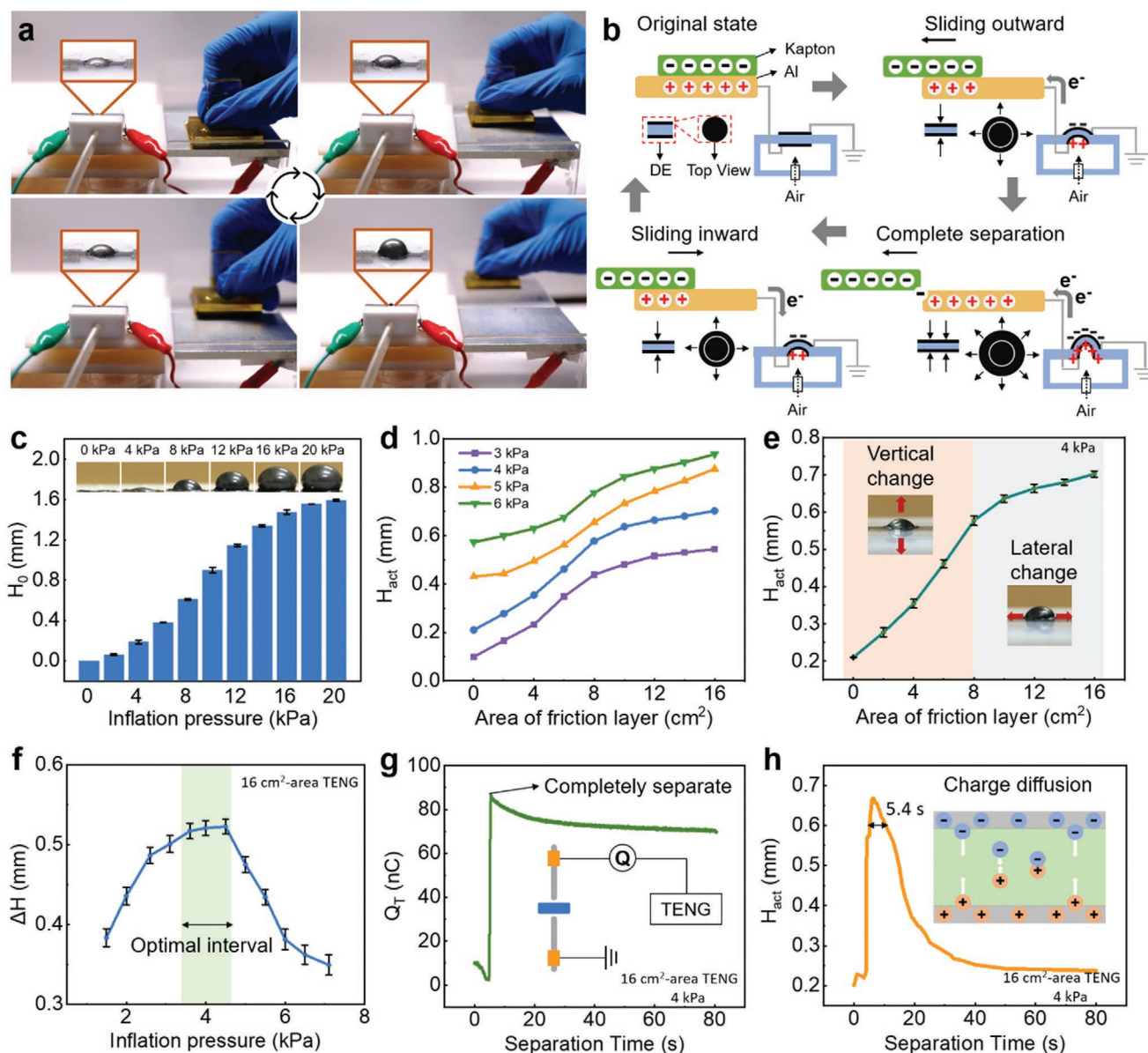


Figure 3. RBDS with single DED. a) Photos of one operation cycle of RBDS. b) Schematic diagram of operation mechanism of RBDS. The Al film is connected to an electrode of the DE membrane, the other electrode of the DE film is grounded, the "black dot" is the top view of the DE membrane. c) Raised height of DED without TENG actuated under different pressure in the chamber. d) Raised height of DED actuated by different area TENG under different pressure in the chamber (3, 4, 5, and 6 kPa). e) Raised height of the DED actuated by different area TENG under 4 kPa pressure in the chamber. f) Raised height difference of DED actuated by 16 cm^2 area TENG under different pressures in the chamber. g) Charge accumulation and release on the DED actuated by 16 cm^2 area TENG under 4 kPa pressures (during original state to completely separated state in Figure 3b), and schematic diagram of test connection. h) Raised height of the DED actuated by 16 cm^2 area TENG under 4 kPa pressures in the chamber, the duration of H_{act} above 0.6 mm was about 5.4 s. (g) and (h) are tested simultaneously.

plane direction. The combined effect of high voltage and air pressure on the DED made it raised as a Braille dot. When the Kapton film fully slid out of the Al foil, the positive charges on the Al foil reached the maximum, leading to the highest voltage loading on the DED and the largest deformation of its morphology. Then the Kapton film was reverted to slide backward and electrons would be transferred from the Al foil to the DED to balance the potential difference between Kapton film and Al

foil. It caused the voltage decrease applied to the DED, then the height of the elastomer dot reduced. When the Kapton film and the Al foil reached the overlapping position completely, the triboelectric charges were equilibrium and the DED returned to its original flat state to refresh the display.

The air pressure in the chamber is one of the critical factors that influence the tactile sensation of the DED. We studied the relationship between the raised height of the DED without

TENG actuated (H_0) and the inflation pressure to find the optimal air pressure (Figure 3c). When the air pressure in the chamber reached to 4 kPa, the DED was raised to 0.2 mm in height, and as the air pressure increased, the H_0 of the DED ascended correspondingly. However, it is not that the higher the initial air pressure, the better the final effect, because the height of the DED actuated by the TENG must also be considered. The raised height of the DED actuated by the TENG (H_{act}) with different areas was compared under different inflation pressure values (3, 4, 5, and 6 kPa), respectively (Figure 3d). Furthermore, we specifically studied the H_{act} of the DED actuated by different areas TENG under 4 kPa inflation pressure (Figure 3e). The DED would have an apparent change in a vertical direction when actuated by the TENG with a small area (less than 8 cm²) under a pressure of 4 kPa in the chamber. That is, when the area of TENG was greater than 8 cm², the H_{act} of the DED began to stabilize.

To verify the actual contributions of the TENG (16 cm² area) to the raised height of the DED, we studied the change of the raised height difference ($\Delta H = H_{act} - H_0$) of the DED under different inflation pressures (Figure 3f). The result showed that when the pressure was about 4 kPa, the ΔH was the largest, which would provide a better tactile sensation. When the two friction layers of the TENG were separated completely, the amount of charge storage reaches the highest value, then the amount of transferred charge decreased as time went on (Figure 3g). The schematic diagram of the test connection is shown in Figure 3g. Correspondingly, the H_{act} of a single DED was also recorded. The height of the DED above 0.6 mm lasted for 5.4 s and then decreased slowly. The possible explanation could be a part of charges diffused and neutralized inside the DE membrane (Figure 3h). The response time for the height change of DED actuated by TENG was only 0.13 s (Figure S8, Supporting Information).

2.4. Refreshable Braille Display System with Six Dielectric Elastomer Dots

The fabrication of the Braille device with six DEDs is mentioned in Experimental Section and Figure 4a. Some experimental results suggest that pre-strain can reinforce the Maxwell stress effect.^[34] In order to find the best strain rate of the dielectric elastomer actuators in the Braille device, we explored the relationship between different strain rate and actuated height of dielectric elastomer actuators (Figure S9, Supporting Information). Considering the actuated height and life span of the dielectric elastomer actuator in the Braille device, a strain rate of 400% is appropriate. Compared to the single DED device, the RBDS with multi-DEDs would be less actuated by the single TENG (16 cm² area, under 4 kPa air pressure in the chamber). The H_{act} of the DEDs gradually degraded with the number of the DEDs increased (Figure 4b). When the single TENG actuated four or more dots of the RBDS simultaneously, the heights were less than 0.6 mm, leading to a weak sensation of touch. To solve this problem, we set multi-TENGs to build an array to actuate the multi-DEDs by one-to-one approach (Figure 4c and Figure S10, Supporting Information), the area of each TENG was 10 cm², the air pressure in the chamber was 4 kPa. Driven

by TENG array, the actuated height of each DED was all about 0.6 mm, which is more stable than the effect by single TENG. Furthermore, the durability of this RBDS was tested by the linear motor with a frequency of 0.5 Hz. After 20 000 cycles of testing, the H_{act} of the DED remained stable, so that the system still had an excellent performance (Figure 4d). Meanwhile, we used a single-pole single-throw (SPST) matrix to adjust the display contents of the RBDS (Figure S11, Supporting Information), showing three Braille letters “A,” “B,” and “C” with single Braille device, respectively (Movie S2, Supporting Information); and three Braille letters “A,” “B,” and “C” with three Braille devices, simultaneously (Figure 4e and Movie S3, Supporting Information). It is worth mentioning that the manual switch used here is for the convenience of operation; then smaller and more controllable electronic switch will be used to control these Braille devices.

2.5. Refreshable Braille Display System with Electronic Switch Controller

To prove the feasibility of the practical application, we designed a program-controlled RBDS with a visible controller (Figure 5a and Movie S4, Supporting Information). The schematic diagram of the connection is shown in Figure 5a. Its internal transistors acted as switches, the open and closed states of the transistors can be controlled by Microprogrammed Control Unit (MCU) with different programs to achieve various characters display using single Braille device (Figure S12, Supporting Information). The results showed that the addition of electronic switches did not significantly reduce the deformation quantity of the DED. In addition, when the TENG slid to the original state, the DED also returned to its initial state to be refreshed. Braille letters of “T,” “E,” “N” and “G” were displayed by the RBDS with different programs, respectively (Figure 5b), which realized the function of refreshable successfully. Hereon, we conceive a future Braille e-book based on the presented RBDS to build Braille devices array actuated by TENGs array. The buttons of the future Braille e-book can realize page changing and function selecting. Furthermore, it can be used to read updatable Braille information from the network (Figure 5c). The corresponding letters in the suppositive Braille e-book were shown in Figure S13, Supporting Information.

3. Conclusion

We have presented a refreshable Braille display system based on TENG and DE membrane. The output voltage generated by TENG reached up to 3.25 kV, which was enough to deform the DE membrane. However, the current generated by TENG was only 2 μ A, it was safe for human body. After adding electronic switches in RBDS, each Braille display module can be controlled by programs to display different Braille characters. The presented Braille device using triboelectric nanogenerator does not require additional HV power supply, which may provide a possibility for the implementation of an easy fabricated, safe and convenient refreshable Braille e-book. Further research will be expected to realize a large-scale

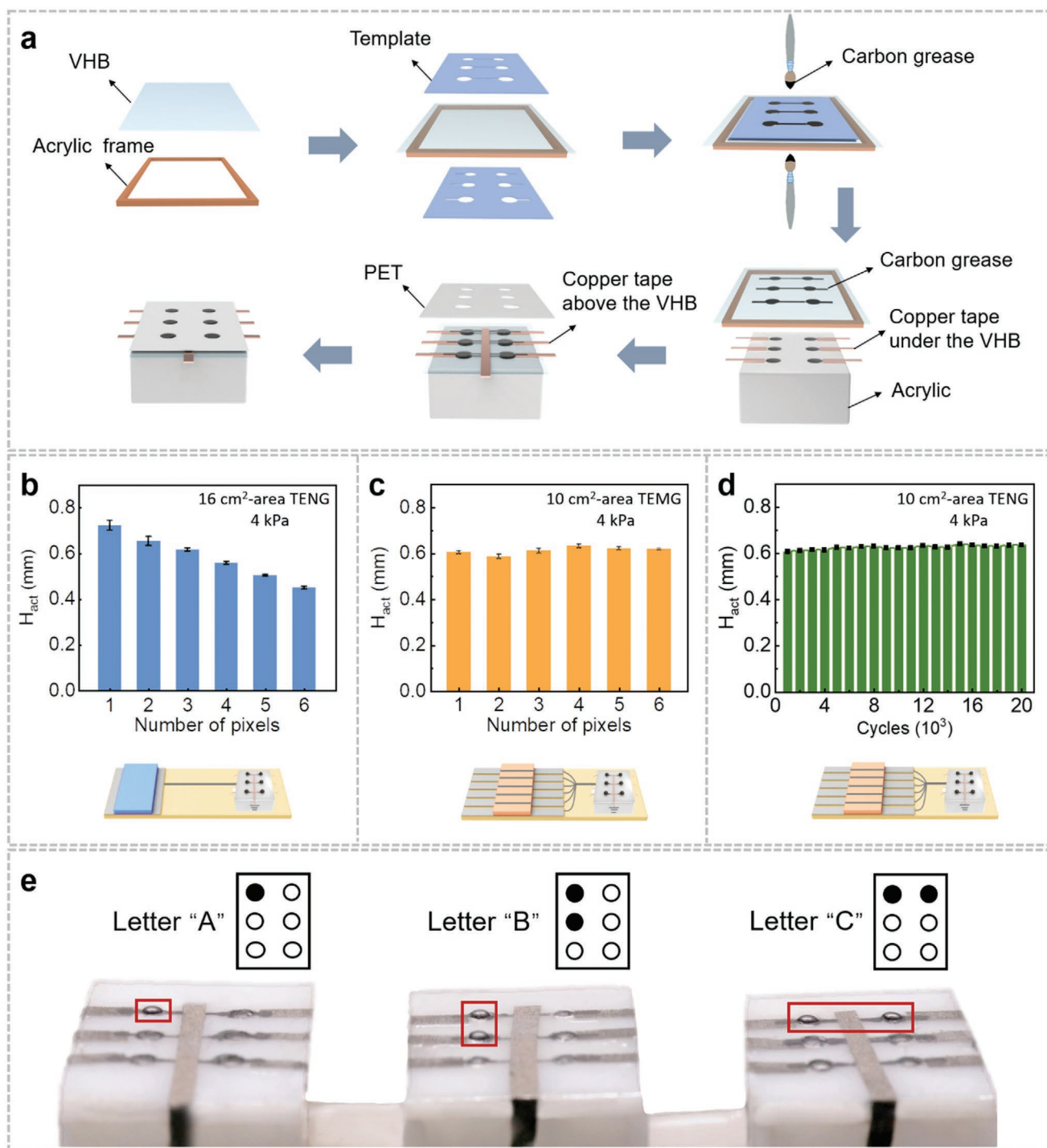


Figure 4. RBDS with six DEDs. a) Fabrication of Braille device with six DEDs. b) H_{act} of DEDs with the number from one to six actuated by single TENG (16 cm² area), simultaneously. c) H_{act} of six DEDs actuated by six corresponding TENGs (10 cm² area). d) Endurance test of RBDS with six DEDs for 20 000 cycles. e) Braille letters of "A," "B," and "C" displayed by three Braille devices with SPST, simultaneously.

Braille devices array, and reduce the size of the whole system, such as modifying the DE membrane to reduce the required actuated voltage, designing TENG as a multilayer array structure, improving the process of TENG to enhance its driving force.

4. Experimental Section

Fabrication of TENG: The TENG was mainly composed of Kapton film, Al foil and acrylic sheet. The fabricated nanostructured Kapton film for the friction layer of TENG was processed by an inductively coupled plasma etching system (SENTECH/SI 500). A piece of 50 μm thick

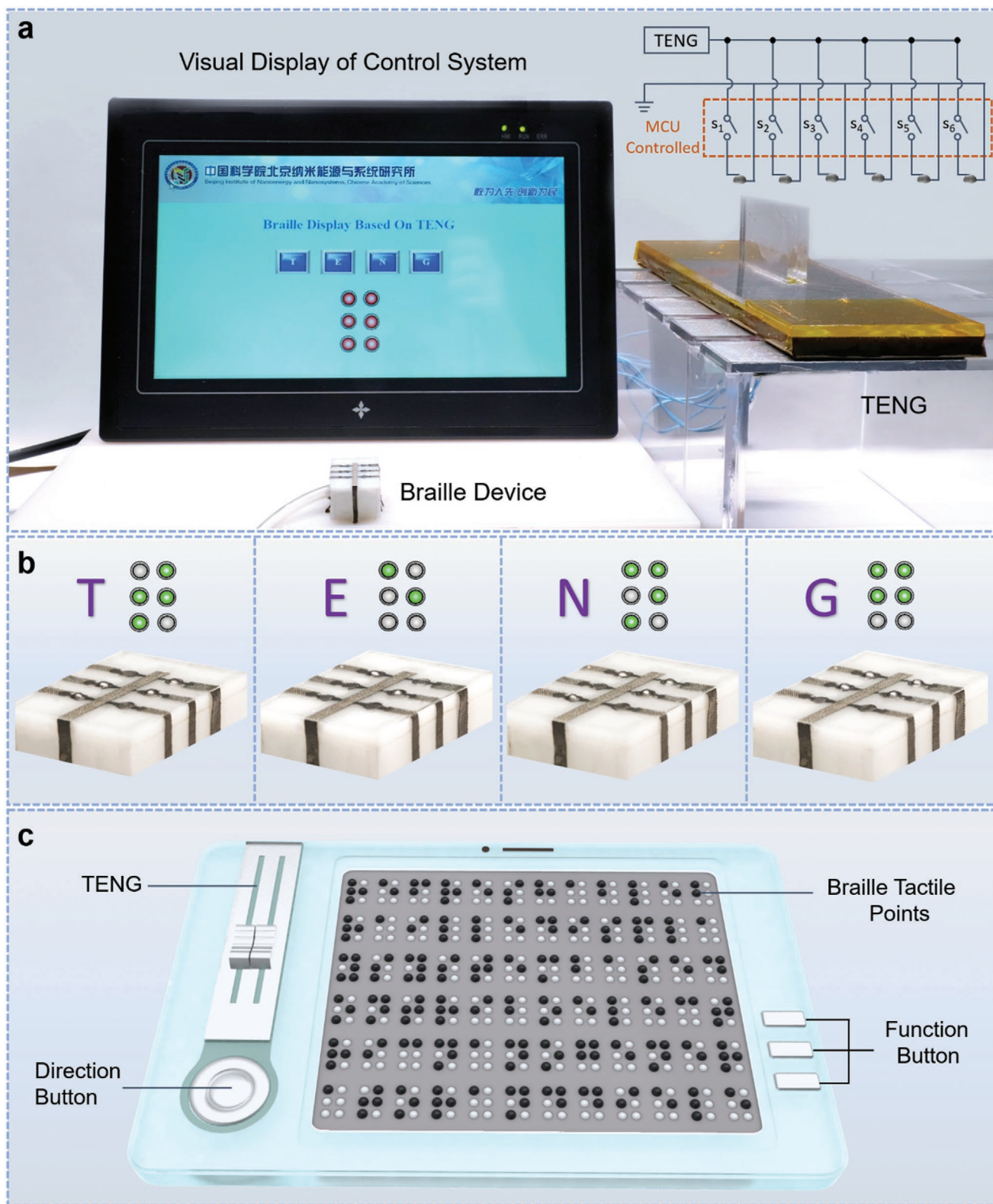


Figure 5. Application and expectation of RBDS with six DEDs. a) Photo of RBDS with visual electronic switch controller, and schematic diagram of the connection. b) Braille letters of “T,” “E,” “N” and “G” displayed by single Braille device with visual electronic switch controller, respectively. c) Refreshable, simple, cost-effective, and safe Braille e-book for the blind in the near future.

Kapton film (American Durafilm) was rinsed with alcohol and deionized water, then, dried with nitrogen gas. The reaction gases Ar, O₂, and CF₄ were introduced into the ICP chamber at a flow rate of 15, 10, and 30 sccm, respectively. This Kapton film was etched by ICP reactive ion etching for 300 s (ICP power: 400 W and 100 W, respectively). The Al foil that acted as the friction layer and electrode was attached on the surface of the acrylic sheet to ensure the surface flatness.

Fabrication of Braille Device: First, DE membrane (VHB 9473, 3M, 0.25 mm thick) was pre-strained by 2 times on the x, y axis (400% strain rate), respectively. Then the membrane was fixed to the acrylic frame for subsequent operations. Next, attach the PTFE templates to both sides of DE membrane, and applied carbon grease to the DE membrane through the templates with a brush to form DED. The copper tape was used to extend the carbon grease electrode. Then, removed the templates, attached the copper tape to the acrylic box, and attached the DE membrane to the box, so that circular conductive carbon grease on the DED was aligned with the round hole in the box, and the square conductive carbon grease under the DE membrane was aligned with the copper tape. Moreover, another layer of copper tape was attached to the square conductive carbon grease above the DE membrane. Finally, cover a PET plate to the device to enhance the bump height of the contact and protect the device. The acrylic frame, PTFE templates, acrylic box and PET plate were cut by laser cutting machine (PLS6.75, Universal). The diameter of the single dot and the full array of Braille dots were 2 mm. The size of the single dot device and the six dot Braille device were both 30 × 22 × 16 mm, and the diameter of the vent hole was 4 mm. The vertical and horizontal distance between two adjacent dots was 4 mm.

Characterization and Measurement: The uniaxial tensile test of the DE membrane was tested by (ESM301, Mark-10). The output performance of TENG was measured and recorded using an electrometer (6514, Keithley; 344-K, TRKE) and oscilloscope (HD 4096, Teledyne LeCroy). In the fatigue test, the TENG was driven periodically by a linear motor (E1100, LinMot, 0.5 Hz frequency). The acrylic sheet with aluminum foil was fixed on the table, and acrylic with Kapton film was attached to the linear motor. The fatigue test was performed for 20 000 cycles. All SEM images were taken with a field emission scanning electron microscope (SU 8020, Hitachi). Optical micrographs were taken with an optical microscope (ECLIPSE LV100ND, Nikon). The height of the contact was recorded by the macro camera (D800, Nikon), and Photoshop for pixel analysis.

Control Module: Programmable Logic Controller (PLCFX1N, Mitsubishi) was used as control module, and internal transistors were used as controllable switches due to their characteristics of fast response (0.2 ms) and long life. Different Braille characters could be converted into switching variables programmatically. The diagram of connection of TENG, Braille device and PLC port is shown in Figure S10, Supporting Information. The common electrode was connected to the ground. PLCFX1N could be extended to 108 ports.

Mechanism of DE Membrane Driven by an Electric Field: For DE membrane with 10–100 μm thickness, the driving voltage of 0.5–10 kV is generally required. The Poisson's ratio of DE is close to 0.5, which means this kind of material is incompressible. The electrostatic force will make the thickness thinner and its area will increase. After the applied electric field is removed, the electrostatic force will disappear, and the DE membrane will return to the original form. However, when the applied voltage exceeds the limit voltage that the material can withstand, the DEA will be broken down. Maxwell force (σ) generated from two opposing electrodes can be expressed as:

$$\sigma = \epsilon_0 \epsilon_r \left(\frac{U}{d} \right)^2 \quad (1)$$

where ϵ_0 is the dielectric constant in vacuum, ϵ_r is the dielectric constant of DE (The relative dielectric constant of DE without pre-straining is about 4.7, and the relative dielectric constant of DE at different pre-strain rates is different), U is the applied voltage and d is the thickness of DE. According to the formula, Maxwell stress (σ) is mainly related to the applied voltage (U) and the thickness of DE (d); therefore, pre-strain the DE membrane to reduce thickness or increasing applied voltage on the DE membrane can significantly increase the electrostatic force.

Supporting Information

Supporting Information is available from the Wiley Online Library or from the author.

Acknowledgements

X.Q., X.M., and B.S. contributed equally to this work. This work was supported by the National Key R&D project from Minister of Science and Technology, China (2016YFA0202703, 2016YFC1102202), National Natural Science Foundation of China (61875015, 11421202, 51775049), the Beijing Natural Science Foundation (7204275, 4192069), Fundamental Research Funds for the Central Universities, and the National Youth Talent Support Program.

Conflict of Interest

The authors declare no conflict of interest.

Keywords

Braille display, dielectric elastomers, refreshable display, self-powered, triboelectric nanogenerator

Received: August 6, 2020
Revised: September 17, 2020
Published online:

- [1] R. R. A. Bourne, S. R. Flaxman, T. Braithwaite, M. V. Cicinelli, A. Das, J. B. Jonas, J. Keeffe, J. H. Kempen, J. Leasher, H. Limburg, K. Naidoo, K. Pesudovs, S. Resnikoff, A. Silvester, G. A. Stevens, N. Tahhan, T. Y. Wong, H. R. Taylor, *Lancet Global Health* **2017**, *5*, e888.
- [2] A. C. Grant, M. C. Thiagarajah, K. Sathian, *Percept. Psychophys.* **2000**, *62*, 301.
- [3] F. Carpi, S. Bauer, D. De Rossi, *Science* **2010**, *330*, 1759.
- [4] A. Marete, A. Poulin, N. Besse, S. Rosset, D. Briand, H. Shea, *Adv. Mater.* **2017**, *29*, 1700880.
- [5] Z. Yu, W. Yuan, P. Brochu, B. Chen, Z. Liu, Q. Pei, *Appl. Phys. Lett.* **2009**, *95*, 192904.
- [6] H. Godaba, C. C. Foo, Z. Q. Zhang, B. C. Khoo, J. Zhu, *Appl. Phys. Lett.* **2014**, *105*, 112901.
- [7] P. Chakraborti, H. A. K. Toprakci, P. Yang, N. Di Spigna, P. Franzon, T. Ghosh, *Sens. Actuators, A* **2012**, *179*, 151.
- [8] Z. Suo, *Acta Mech. Solida Sin.* **2010**, *23*, 549.
- [9] W. Gu, X. Y. Zhu, N. Futai, B. S. Cho, S. Takayama, *Proc. Natl. Acad. Sci. USA* **2004**, *101*, 15861.
- [10] G. Bogda, B. Vishoot, C. Grider, D. Schroeder, *J. Eng. Technol.* **2011**, *28*, 26.
- [11] R. E. Fan, A. M. Feinman, C. Wottawa, C.-H. King, M. L. Franco, E. P. Dutton, W. S. Grundfest, M. O. Culjat, in *Medicine Meets Virtual Reality 17 – Nextmed: Design for/the Well Being*, Vol. 142 (Eds: J. D. Westwood, S. W. Westwood, R. S. Haluck, H. M. Hoffman, G. T. Mogel, R. Phillips), IOS Press, Amsterdam **2009**, p. 94.
- [12] F. Basciftci, A. Eldem, *Displays* **2016**, *41*, 33.
- [13] R. Hinchet, H.-J. Yoon, H. Ryu, M.-K. Kim, E.-K. Choi, D.-S. Kim, S.-W. Kim, *Science* **2019**, *365*, 491.
- [14] S. Gao, R. Wang, C. Ma, Z. Chen, Y. Wang, M. Wu, Z. Tang, N. Bao, D. Ding, W. Wu, F. Fan, W. Wu, *J. Mater. Chem. A* **2019**, *7*, 7109.
- [15] H. Yang, M. Deng, Q. Tang, W. He, C. Hu, Y. Xi, R. Liu, Z. L. Wang, *Adv. Energy Mater.* **2019**, *9*, 1901149.

- [16] X. Cheng, W. Tang, Y. Song, H. Chen, H. Zhang, Z. L. Wang, *Nano Energy* **2019**, *61*, 517.
- [17] Y. Zou, P. Tan, B. Shi, H. Ouyang, D. Jiang, Z. Liu, H. Li, M. Yu, C. Wang, X. Qu, L. Zhao, Y. Fan, Z. L. Wang, Z. Li, *Nat. Commun.* **2019**, *10*, 2695.
- [18] M. Wang, J. Zhang, Y. Tang, J. Li, B. Zhang, E. Liang, Y. Mao, X. Wang, *ACS Nano* **2018**, *12*, 6156.
- [19] X. Pu, H. Guo, Q. Tang, J. Chen, L. Feng, G. Liu, X. Wang, Y. Xi, C. Hu, Z. L. Wang, *Nano Energy* **2018**, *54*, 453.
- [20] G.-T. Hwang, H. Park, J.-H. Lee, S. Oh, K.-I. Park, M. Byun, H. Park, G. Ahn, C. K. Jeong, K. No, H. Kwon, S.-G. Lee, B. Joung, K. J. Lee, *Adv. Mater.* **2014**, *26*, 4880.
- [21] H. Ouyang, Z. Liu, N. Li, B. Shi, Y. Zou, F. Xie, Y. Ma, Z. Li, H. Li, Q. Zheng, X. Qu, Y. Fan, Z. L. Wang, H. Zhang, Z. Li, *Nat. Commun.* **2019**, *10*, 1821.
- [22] J. Wang, H. Wang, T. He, B. He, N. V. Thakor, C. Lee, *Adv. Sci.* **2019**, *6*, 1900149.
- [23] X. Chen, Z. Ren, H. Guo, X. Cheng, H. Zhang, *Appl. Phys. Lett.* **2020**, *116*, 043902.
- [24] F.-R. Fan, Z.-Q. Tian, Z. L. Wang, *Nano Energy* **2012**, *1*, 328.
- [25] Z. L. Wang, *Mater. Today* **2017**, *20*, 74.
- [26] X. Chen, T. Jiang, Y. Yao, L. Xu, Z. Zhao, Z. L. Wang, *Adv. Funct. Mater.* **2016**, *26*, 4906.
- [27] A. Li, Y. Zi, H. Guo, Z. L. Wang, F. M. Fernandez, *Nat. Nanotechnol.* **2017**, *12*, 481.
- [28] M.-C. Wong, W. Xu, J. Hao, *Adv. Funct. Mater.* **2019**, *29*, 1904090.
- [29] J. Cheng, W. Ding, Y. Zi, Y. Lu, L. Ji, F. Liu, C. Wu, Z. L. Wang, *Nat. Commun.* **2018**, *9*, 3733.
- [30] Y. Yang, H. Zhang, J. Chen, Q. Jing, Y. S. Zhou, X. Wen, Z. L. Wang, *ACS Nano* **2013**, *7*, 7342.
- [31] W. Liu, Z. Wang, G. Wang, G. Liu, J. Chen, X. Pu, Y. Xi, X. Wang, H. Guo, C. Hu, Z. L. Wang, *Nat. Commun.* **2019**, *10*, 1426.
- [32] G. Zhu, J. Chen, T. Zhang, Q. Jing, Z. L. Wang, *Nat. Commun.* **2014**, *5*, 3426.
- [33] Q. Zheng, Y. Jin, Z. Liu, H. Ouyang, H. Li, B. Shi, W. Jiang, H. Zhang, Z. Li, Z. L. Wang, *ACS Appl. Mater. Interfaces* **2016**, *8*, 26697.
- [34] Z. Cheng, Q. Zhang, *MRS Bull.* **2008**, *33*, 183.